



UDC 678.023

## NUMERICAL STUDY OF NONISOTHERMAL FLOW OF POLYMER MELT WITH UNDERMELTED GRANULES IN AN ANNULAR CHANNEL OF A DISK EXTRUDER

Volodymyr Novodvorskyi; Georgiy Ivanitsky; Nikolai Shved

*National Technical University of Ukraine «Igor Sikorsky Kyiv Polytechnic Institute», Kyiv, Ukraine*

**Summary.** A computational experiment was carried out on the basis of the created model of melt flow with undermelted granules in a straight annular channel, which takes into account the design characteristics of a pilot-industrial disk extruder. A polymer composition based on high-pressure polyethylene (PE 15803-020) was chosen as a model object. The calculation procedure is presented in an analytical form at disk speeds of minimum value – 120, nominal value – 150, and maximum value – 180 rpm.

**Key words:** disk extruder; polymers, annular channels, modeling, non-isothermal processes, melting/

[https://doi.org/10.33108/visnyk\\_tntu2023.04.115](https://doi.org/10.33108/visnyk_tntu2023.04.115)

Received 13.10.2023

**Introduction.** Polymer products are widely used in various industries due to their unique properties. These properties can be obtained if good mixing of the melt is ensured. The homogenization zone is responsible for ensuring good mixing of the melt.

An effective equipment that achieves a high level of mixing at a low pressure drop and consequently low energy consumption is a disk extruder [1–3]. However, the processes occurring in the channels of the homogenization zone of a disk extruder have not yet been sufficiently studied.

The homogenization process in each channel of the homogenization zone of a disk extruder is different. The following main directions characterize the study of extrusion processes in the homogenization zone of a disk extruder:

1. Modeling of hydrodynamic and thermal processes in non-Newtonian fluid flow
  - in the straight annular channel of the homogenization zone [4];
  - in the conical annular channel of the homogenization zone;
  - in the disk gap of the homogenization zone [1–3, 5].
2. Analyze and select the optimal parameters of the disk gap and disk speed;
3. Create a general procedure for calculating the channels of the homogenization zone.

In the paper [5], the homogenization zone is described as a sequence of several separate channels (Figure 1). The straight cylindrical annular channel begins immediately after the screw cutting of the extruder. Processes of melt homogenization in this and the following channels of the dosing zone are described in detail in works [4, 5]. Good melt quality can be obtained when both mechanical and temperature homogeneities have been achieved in the dosing zone. Settings of the parameters of the homogenization process, which affect the quality of the melt, were considered in works [6–8]. In work [4], based on the theoretical analysis of hydrodynamic, thermal and rheological processes, accompanying the flow of the polymer melt in the straight ring zone, a general procedure for calculating all three channels of the homogenization zone, shown in Figure 1, is proposed.

The non-isothermal behavior of the flow of highly viscous polymer melts through the narrow annular channels of extruders is caused, first of all, by the excessively high intensity of

energy dissipation, associated with the high frequency of rotation of the screw and, accordingly, with high shear stress values, as well as by the heat exchange of the melt with cooled or heated channel walls [3, 9, 10].

In the non-isothermal mode, both in the first and second annular channels of the homogenization zone, shown in Figure 1, intensive processes of granule melting and mixing of the melt simultaneously, which ensures a high of homogenization degree of the melt. The melting of granules in the middle of the annular channels can be completed even before the transition of the melt into the disk gap. Until now, the regularities of the flow of these compatible processes in annular channels remain practically unstudied because of lack of rigorous information.

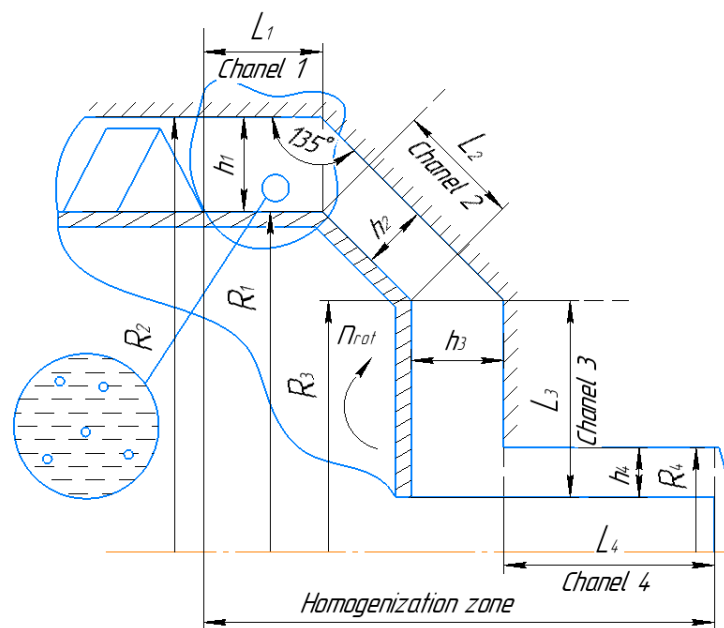


**Figure 1.** Schematic image n of the homogenization zones of the disk extruder

Therefore, there is a need for a study for the operation of disk extruders that allows the development of a flexible and controllable homogenization process with the ability to determine and regulate good melt quality when the machine is running at a constant output.

The results of this work will be used to further study the non-isothermal processes of melt flow and granule melting in the conical annular zone and in the disk zone.

**The objective of the research** is to study the nonisothermal process of melt flow containing a certain amount of undermelted granules, to describe the process of heating and melting of granules due to the dissipation energy of the channels of the homogenization zone.

**Statement of the problem.** Let us consider the non-isothermal steady flow of polymer melt in a straight annular channel between two coaxial cylinders, of which the inner cylinders with radius  $R_1$  rotates with an angular speed  $\omega_0$ , and the outer one with radius  $R_2$  is stationary. The total dimensions of the annular channel are the channel length  $L_1$ , gap width  $h_r = R_2 - R_1$  and cross-sectional area  $S_r = \pi(R_2^2 - R_1^2)$ . The flow of the melt along the axial direction occurs due to the influence of the pressure gradient, which for a non-isothermal behavior is a variable value ( $dp/dz = f(z)$ ). The problem is solved in the cylindrical coordinate system  $(z, r, \theta)$ .

The polymer melt, which is a non-Newtonian pseudo-plastic liquid with known rheological characteristics, contains a certain number of monodisperse undermelted polymer granules with an initial radius  $R_{gr0}$ , which are uniformly placed in the volume of the melt. The concentration of granules per unit volume of the mixture  $n_{gr} = \text{const}$ . Therefore, the initial volume fraction of polymer granules is determined as  $V_{gr0} = 4/3 \pi R_{gr0}^3 \cdot n_{gr}$  and measured in  $\text{m}^3/\text{m}^3$ . The melting temperature  $T_m$ , at which the polymer completely transits from solid state to liquid one, is known. The melt temperature at the entrance to the channel is equal to  $T_{l0}$ . The initial volume-averaged temperature of all granules  $\bar{T}_{gr0}$  is the same and is defined as  $\bar{T}_{gr0} < T_m < T_{l0}$ . It is assumed that in the investigated temperature range the density of the solid phase of the granules with an error of up to 3% is equal to the density of the polymer melt  $\rho_l$  [1, 2, 11].

When the inner cylinder rotates in the viscous liquid, frictional forces arise, that act between each pair of adjacent cylindrical layers of the melt, as a result of which the mechanical energy is transformed into thermal one and the melt is heated due to viscous dissipation [9–12]. Without limiting the generality, we will assume that the surface temperature of the channel walls at each part of the gap is equal to the current temperature of the melt, that is, the process proceeds in the adiabatic mode. In the process of melting granules inside the channel, their volume fraction decreases and, accordingly, the volume fraction of the melt increases.

It is necessary to determine the change in pressure  $p_z = f(z)$ , the mean temperature of the melt  $\bar{T}_l = f(z)$ , the effective viscosity of the melt  $\mu_{ef} = f(z)$ , the volume-averaged temperature of the granules  $\bar{T}_{gr} = f(z)$  and the volume fraction of the granules  $V_{gr} = f(z)$  along the length of the channel.

**Calculation of the melt temperature.** The enthalpy of the mixture of melt with granules consists of the melt enthalpy and the solid grain enthalpy. Then the amount of enthalpy entering per unit time with the mixture flow through the flat annular surface with coordinate  $\zeta$  is determined as

$$H_z = \rho_l c_l \bar{v}_z S_r \cdot \left\{ \left[ (T_l - T_{st}) \cdot (1 - V_{gr}) \right]_{\zeta} + \frac{\bar{c}_s}{c_l} \left[ (\bar{T}_{gr} - T_{st}) \cdot V_{gr} \right]_{\zeta} \right\}. \quad (1)$$

Here  $T_{st}$  is an arbitrarily chosen reference temperature;  $\bar{v}_z = G_V / S_r$  is the mean velocity of the axial melt flow; the melt density  $\rho_l$  and the specific heat capacity of the melt  $c_l$  are taken as constant values independent of temperature [2, 8, 11];  $\bar{c}_s$  is the average specific heat capacity of a solid granule in the temperature range of  $\bar{T}_{gr0} \div T_m$ .

In the absence of external heat sources, the enthalpy of the mixture during its passage through the channel remains constant. Therefore, there is no enthalpy change in the section of the channel  $\Delta z$  from  $\zeta$  to  $\zeta + \Delta z$  and the heat balance equation is written as

$$\Delta H_{\Delta z} \equiv \rho_l c_l \bar{v}_z S_r \cdot \left\{ \left[ T_l \cdot (1 - V_{gr}) \right]_{\Delta z} + \frac{\bar{c}_s}{c_l} \cdot \left[ \bar{T}_{gr} \cdot V_{gr} \right]_{\Delta z} \right\} = 0. \quad (2)$$

After obvious transformations, equation (2) reduces to the form

$$\Delta H_{\Delta z} = \rho_l c_l \bar{v}_z S_r \cdot \left[ (\Delta T_l)_{\Delta z} - \Delta(T_l \cdot V_{gr})_{\Delta z} + \frac{\bar{c}_s}{c_l} \cdot \Delta(\bar{T}_{gr} \cdot V_{gr})_{\Delta z} \right]. \quad (3)$$

The right side of equation (3) is equal to zero. It follows that in the absence of external heat sources, the melt enthalpy in the cross-sectional area  $\Delta z$  decreases due to its consumption for melting and heating the granules. Accordingly, the enthalpy of the granules increases. In the presence of viscous dissipation, the heat balance equation must be written taking account of the fact that the liquid melt per unit volume occupies only a part of the volume equal to  $(1 - V_{gr})$ . Then the amount of dissipation energy entering the layer  $\Delta z$  with the volume  $S_r \Delta z$  per unit time (or the power of dissipation) is described by the equation [12]

$$\Delta H_{dis} = \mu_{ef}(T) \cdot (\dot{\gamma}_{rz}^2 + \dot{\gamma}_{r\theta}^2) \cdot (1 - V_{gr}) \cdot S_r \Delta z, \quad (4-a)$$

or by identical to it equation

$$\Delta H_{dis} = K_T \cdot \left[ (\dot{\gamma}_{rz}^2 + \dot{\gamma}_{r\theta}^2) \right]^{\frac{1+n}{2}} \cdot (1 - V_{gr}) \cdot S_r \Delta z. \quad (4-b)$$

Here  $\mu_{ef}(T)$  is the effective viscosity of the melt, which for a pseudo-plastic liquid is described by the Oswald–de Weyle power law;  $\dot{\gamma}_{rz} = dv_z/dr$  is shear rate of the axial flow;  $\dot{\gamma}_{r\theta} = dv_\theta/dr$  is shear rate of the tangential (circular) flow;  $K_T = f(T)$  is consistency coefficient;  $n = f(T)$  is exponent.

As shown by our previous studies [4], the shear rate of the axial flow  $\dot{\gamma}_{rz}$  is negligibly lower than that of the tangential flow  $\dot{\gamma}_{r\theta}$  and it can be neglected, what shall be used in further calculations.

Obviously, the change in the mixture enthalpy  $\Delta H_{\Delta z}$  at any section of the channel is equal to the value of the dissipation power  $q_{dis}$  at this section.

Taking into account equations (3) and (4-a), the heat balance equation in a layer  $\Delta z$  in the presence of heat dissipation can be written as

$$\rho_l c_l \bar{v}_z S_r \left[ (\Delta T_l)_{\Delta z} - \Delta(T_l V_{gr})_{\Delta z} + \frac{\bar{c}_s}{c_l} \Delta(\bar{T}_{gr} \cdot V_{gr})_{\Delta z} \right] = \mu_{ef}(T) \cdot \dot{\gamma}_{r\theta}^2 (1 - V_{gr}) S_r \Delta z. \quad (5)$$

After dividing both parts of equation (5) by  $S_r \Delta z$  and passing to the limit  $\Delta z \rightarrow 0$ , the equation is reduced to the form

$$\rho_l c_l \bar{v}_z \cdot \left[ \frac{dT_l}{dz} - \frac{d(T_l \cdot V_{gr})}{dz} + \frac{\bar{c}_s}{c_l} \cdot \frac{d(\bar{T}_{gr} \cdot V_{gr})}{dz} \right] = \mu_{ef}(T) \cdot \dot{\gamma}_{r\theta}^2 \cdot (1 - V_{gr}). \quad (6)$$

Differentiating the product in both derivatives in square brackets on the right-hand side of equation (6) and performing the obvious transformations, one can obtain equation with respect to the melt temperature

$$\frac{dT_l}{dz} = \frac{1}{(1-V_{gr}) \cdot c_l} \left[ \frac{\mu_{ef}(T) \cdot \dot{\gamma}_{r\theta}^2 \cdot (1-V_{gr})}{\rho_l \bar{v}_z} + \bar{c}_s \cdot (T_l - \bar{T}_{gr}) \frac{dV_{gr}}{dz} - \bar{c}_s V_{gr1} \frac{d\bar{T}_{gr}}{dz} \right]. \quad (7)$$

The rate of change in the granules volume during their melting  $dV_{gr}/dz$  is a negative value, so the second term in square brackets is also negative.

The enthalpy change in the melting process, which is represented by the second term on the right side of the equation (7), can be represented in the form of two components

$$\bar{c}_s \cdot (T_l - \bar{T}_{gr}) \cdot \frac{dV_{gr}}{d\tau} = [c_l \cdot (T_l - T_m) + \bar{c}_s \cdot (T_m - \bar{T}_{gr})] \cdot \frac{dV_{gr}}{d\tau}. \quad (8)$$

The second term in square brackets on the right hand side of (8) defines the enthalpy change associated with heating the surface layer of the granule to the melting temperature  $T_m$ . In fact, this is «hidden heat of polymer melting», which is not consumed at a given melting point, as in the case of a phase transition of the first kind, but gradually – in the temperature interval  $(T_m \div \bar{T}_{gr})$ . The first term in square brackets in the right side of (8) determines the change in enthalpy associated with further heating of the already completely melted polymer from  $T_m$  to the current temperature of the surrounding melt  $T_l(\tau)$ . Taking this into account, the change in the melt temperature along the length of the channel can be represented as

$$\frac{dT_l}{dz} = \frac{1}{(1-V_{gr}) \cdot c_l} \left\{ \frac{\mu_{ef}(T) \cdot \dot{\gamma}_{r\theta}^2 \cdot (1-V_{gr})}{\rho_l \bar{v}_z} + [c_l \cdot (T_l - T_m) + \bar{c}_s \cdot (T_m - \bar{T}_{gr})] \frac{dV_{gr}}{dz} - \bar{c}_s \cdot V_{gr1} \frac{d\bar{T}_{gr}}{dz} \right\}. \quad (9)$$

The first term in the brace brackets in the right side of (9) is the dissipation power, written through the effective viscosity  $\mu_{ef}$ , according to the equation (4-a). Dissipation power can be also determined from equation (4-b) through the consistency coefficient  $K_T$ . Substituting this value into equation (9), one obtains the identical heat balance equation.

Equation (9) contains three unknown variables that depend on the coordinate  $z$ . These are the melting temperature  $T_l$ , the total granule volume  $V_{gr}$  and the volume-averaged temperature of the granules  $\bar{T}_{gr}$ . To determine the last two parameters, we need two more equations describing the dependences  $V_{gr} = f(z)$  and  $\bar{T}_{gr} = f(z)$ .

**Calculation of the granule melting rate.** During passing the polymer mixture through the channel, from the melt with the current temperature  $T_l(z)$  to the surface of the granules with constant temperature  $T_m$  heat enters, which is spent on melting the surface layer of the granules and on their heating, that is, increasing their average

temperature  $\bar{T}_{gr}$ . If the melting rate of single granule is set equal to  $dm_{gr1}/d\tau = \rho_{gr} dV_{gr1}/d\tau$ , then the melting rate of a totality of monodisperse granules can be determined from the heat transfer equation

$$4\pi R_{gr1} \lambda_l (T_l - T_m) n_{gr} = 4\pi R_{gr1}^2 \frac{dR_{gr1}}{dz} n_{gr} \rho_l \bar{c}_s (T_m - \bar{T}_{gr}) \bar{v}_z + 4\pi R_{gr1} \lambda_s (T_m - \bar{T}_{gr}) n_{gr}.$$

The left side of this equation is the amount of heat transferred from the melt to the granule surface due to thermal conductivity. The first term in the right side of (10) is the amount of input heat that is spent on melting the surface layer of granules. The second term is the amount of input heat used to heat the granules. Here  $\lambda_l$  and  $\lambda_s$ , are, respectively, the thermal conductivity of the melt and granules, which in the studied temperature range can be considered as temperature-independent values [2, 4, 9, 11].

The heat transfer equation can be written not through the radius of an individual granule  $R_{gr1}$ , but through the total volume of granules  $V_{gr}$ , using the relations

$$4\pi R_{gr1} = \left( \frac{3V_{gr}}{4\pi n_{gr}} \right)^{0,33} = 7,8 \cdot \left( \frac{V_{gr}}{n_{gr}} \right)^{0,33} \quad \text{and} \quad 4\pi R_{gr1}^2 \frac{dR_{gr1}}{dz} n_{gr} = \frac{dV_{gr}}{dz}. \quad (10)$$

Then the heat transfer equation is reduced to the form

$$\rho_l \cdot c_s (T_m - \bar{T}_{gr}) \cdot \bar{v}_z \frac{dV_{gr}}{dz} = 7,8 \cdot \left( \frac{V_{gr}}{n_{gr}} \right)^{0,33} n_{gr} \cdot [\lambda_l (T_l - T_m) - \lambda_s \cdot (T_m - \bar{T}_{gr})]. \quad (11)$$

Solving this equation with respect to  $dV_{gr}/dz$ , one obtains the differential equation for the melting rate of granules in the melt flow per unit length of the channel

$$\frac{dV_{gr}}{dz} = - \frac{7,8 \cdot (V_{gr}/n_{gr})^{0,33} \cdot n_{gr}}{\rho_l \cdot c_s (T_m - \bar{T}_{gr}) \cdot \bar{v}_z} \cdot [\lambda_l (T_l - T_m) - \lambda_s (T_m - \bar{T}_{gr})]. \quad (12)$$

As a result, a differential equation for the dependence  $V_{gr} = f(z)$  is obtained.

**Calculation of the volume-averaged temperature of the granules.** According to equation (10), from the total amount of heat coming from the melt to the granules in a section  $dz$ , part of the heat is spent on increasing volume-averaged temperature of the granules  $\bar{T}_{gr}$ .

$$4\pi R_{gr1} \cdot (T_m - \bar{T}_{gr}) \cdot n_{gr} = \rho_l \cdot \bar{c}_s \cdot \bar{v}_z \cdot \left( \frac{4}{3} \pi R_{gr1}^3 \right) \cdot \frac{d\bar{T}_{gr}}{dz} \cdot n_{gr}. \quad (13)$$

After reduction in both parts of (13), the equation can be rewritten as

$$\frac{d\bar{T}_{gr}}{d\tau} = \frac{3\lambda_s \cdot (T_m - \bar{T}_{gr})}{\rho_l \bar{c}_s \cdot \bar{v}_z \cdot R_{gr1}^2}. \quad (14)$$

Substituting first of relations (10) into equation (14) yields

$$\frac{d\bar{T}_{gr}}{dz} = \frac{3\lambda_s \cdot (T_m - \bar{T}_{gr})}{0,384 \cdot (V_{gr}/n_{gr})^{0,66} \cdot \rho_l \cdot \bar{c}_s \cdot \bar{v}_z}. \quad (15)$$

As a result, a differential equation for the dependence  $\bar{T}_{gr} = f(z)$  is obtained.

**System of model equations** includes three differential equations, which under given boundary conditions describe the changes in the mean melt temperature  $T_l = f(z)$ , in the volume-averaged granule temperature  $\bar{T}_{gr} = f(z)$ , and in the total granule volume  $V_{gr} = f(z)$ , when a polymer melt passes through a straight annular channel. The system of equations also includes an additional independent differential equation, which describes the distribution of axial pressure in the melt  $p = f(z)$  along the channel length. The derivation of the last equation is considered in detail in [4].

1. Melt temperature equation written through the consistency coefficient

$$\frac{dT_l}{dz} = \frac{1}{(1-V_{gr})c_l} \left\{ \frac{\mu_{ef}(T) \cdot \dot{\gamma}_{r\theta}^2 (1-V_{gr})}{\rho_l \bar{v}_z} + [c_l(T_l - T_m) + c_s(T_m - \bar{T}_{gr})] \frac{dV_{gr}}{dz} - \bar{c}_s V_{gr1} \frac{d\bar{T}_{gr}}{dz} \right\}, \quad (16)$$

is solved under the boundary condition:  $T_l(0) = T_0$ .

2. The equation for changing the total granule volume in the mixture

$$\frac{dV_{gr}}{dz} = - \frac{7,8 \cdot (V_{gr}/n_{gr})^{0,33} \cdot n_{gr}}{\rho_l \cdot c_s (T_m - \bar{T}_{gr}) \cdot \bar{v}_z} \cdot [\lambda_l(T_l - \bar{T}_m) - \lambda_s(T_m - \bar{T}_{gr})], \quad (17)$$

is solved under the boundary condition:  $V_{gr}(0) = V_{gr0}$ .

3. Equation of the volume-average temperature of the granules

$$\frac{d\bar{T}_{gr}}{dz} = \frac{3\lambda_s \cdot (T_m - \bar{T}_{gr})}{0,384 \cdot (V_{gr}/n_{gr})^{0,66} \cdot \rho_l \cdot \bar{c}_s \cdot \bar{v}_z}, \quad (18)$$

is solved under the boundary condition:  $\bar{T}_{gr}(0) = \bar{T}_{gr0}$ .

4. Pressure gradient equation in the channel

$$\frac{dp}{dz} = - \frac{2K_T \cdot (G_V)^n}{(R_1 + R_2)^n \cdot (h_r/2)^{1+2n}} \left( \frac{1+2n}{2\pi m} \right)^n, \quad (19)$$

is solved under the boundary condition:  $p(0) = p_0$ .

In addition to differential equations, the model also includes algebraic equations that describe:

- Dependence of the consistency coefficient  $K_T$  on temperature

$$K_T(T) = K_{T0} \cdot \exp[-\beta \cdot (T_l - T_{st})], \quad (20)$$

where  $K_{T0} = K_T(T_{st})$  and  $\beta$  is a temperature coefficient of viscosity.

- Dependence of effective viscosity on temperature

$$\mu_{ef}(T) = K_T(T) \cdot (\gamma_{r\theta})^{n-1}. \quad (21)$$

- Dependence of the exponent on temperature

$$n = n_0 + \alpha_n (T_l - T_{st}), \quad (22)$$

where  $n_0 = n(T_{st})$  and  $\alpha_n$  is a temperature coefficient.

**Analysis of the research results.** On the basis of the created model of melt flow with undermelted granules in a straight annular channel at the exit from the screw section of the extruder, a computational experiment was conducted taking account of the design characteristics and operational parameters of the industrial disk extruder [3, 5]. The length of the annular gap  $L_1 = 10$  mm, width  $h_r = 5$  mm. The radius of the rotating cylinder  $R_1 = 87.5$  mm, the radius of the outer cylinder  $R_2 = 92.5$  mm. The research was conducted at three values of screw revolution speed: 120, 150 and 180 rpm (respectively, at angular velocities  $\omega_0$  of  $12.5 \text{ s}^{-1}$ ,  $15.7 \text{ s}^{-1}$  and  $18.8 \text{ s}^{-1}$ ).

A polymer composition based on high-pressure polyethylene (LDPE 15803-020 brand) was chosen as a model object. Table 1 presents physical and rheological properties of this polymer composition. In the temperature range of  $T_l > T_m$ , the heat capacity of the melt  $c_l(T)$  changes slightly. Therefore, to estimate the melt heat capacity  $c_l$ , its average value was taken in the melt temperature range  $T_m < T_l \leq 200^\circ\text{C}$ . This interval corresponds to the temperature range in the dosing zone of extruders [7, 9]. The values of density and thermal conductivity, given in the Table 1, were determined based on the same considerations. The mean heat capacity value of the granules  $\bar{c}_s$ , as well as the value of the melting temperature  $T_m$ , were selected based on the analysis of literature data for high-pressure polyethylene [2, 8, 11]. A power law was used to describe the dependence of the effective viscosity on the shear rate. The standard temperature was taken to be  $T_{st} = 160^\circ\text{C}$ .

**Table 1**

Rheological and physical properties of the polymer

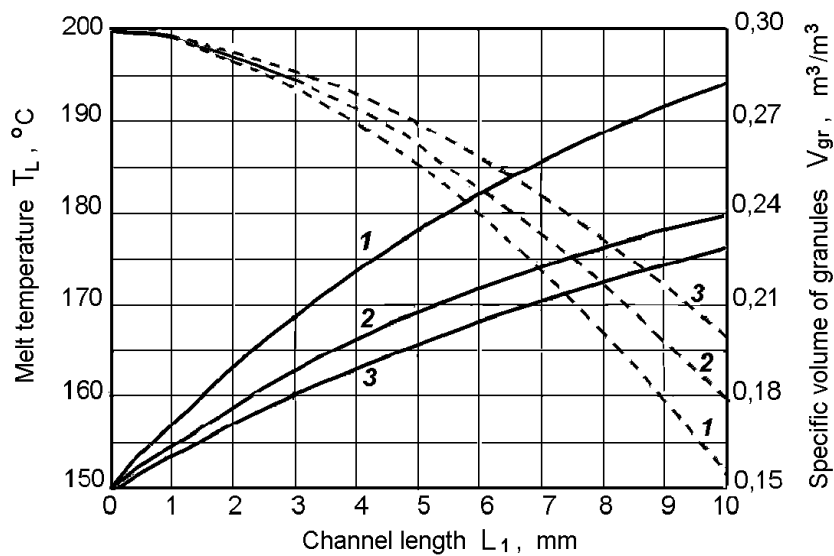
$K_{T0}$	$n_0$	$\beta$	$\rho_l$	$T_m$	$c_l$	$\bar{c}_s$	$\lambda_l$	$\lambda_s$
Pa·s <sup>n</sup>	–	1/K	kg/m <sup>3</sup>	°C	J/kg·K	J/kg·K	J/m <sup>s</sup> ·K	J/m <sup>s</sup> ·K
23750	0,34	0,0172	910	120	2484	9935	0,235	0,300



The melt, containing the granules, move through the annular channel at a constant volumetric flow  $G_V = 9.06 \cdot 10^{-6} \text{ m}^3/\text{s}$  with mean axial velocity  $\bar{v}_z = 3.2 \text{ mm/s}$  under the influence of melt pressure at the channel entrance  $p_0 = 5 \text{ MPa}$ .

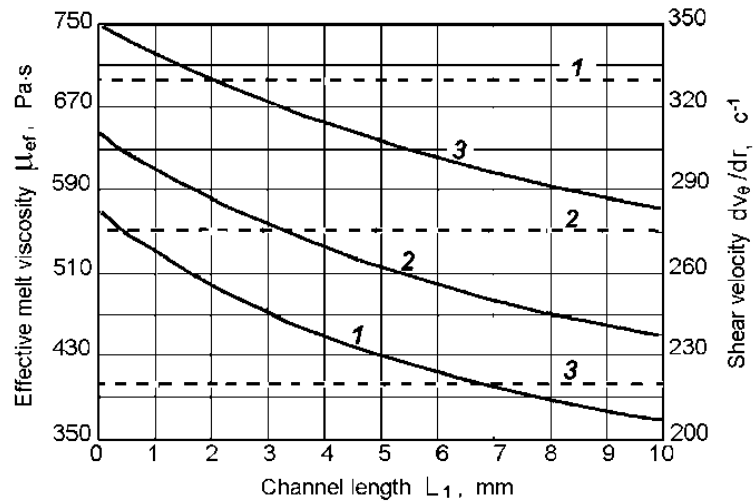
It has been found in previous studies that the centrifugal pressure, arising in the gap on account of the inner cylinder rotation, changes by no more than 4% across the width of the gap [4]. The centrifugal pressure value at any point of the gap is negligibly small compared to the axial pressure value. Calculations also showed that for this type of extruder, in a wide range of changes in operating parameters, the shear rate of the axial flow  $\dot{\gamma}_{rz}$  is two orders of magnitude lower than that of the circular flow  $\dot{\gamma}_{r\theta}$ . Therefore, the dissipation intensity  $q_{dis} \propto \dot{\gamma}_{rz}^2 + \dot{\gamma}_{r\theta}^2$  depends exclusively on the shear rate of the circular flow, which, in turn, depends on the rotation frequency ( $\dot{\gamma}_{r\theta} = \omega_0 R_1 / h_r$ ). According to equations (16) and (17), the rate of change in the melt temperature and the rate of the granules melting along the channel length should depend on the frequency of rotation of the inner cylinder.

Figure 2 shows that the higher the rotation frequency  $\omega_0$ , the stronger increasing the melt temperature and the faster the decreasing the volume of the granules.



**Figure 2.** Distribution of the melt temperature  $T_l = f(z)$  (solid lines) and the specific volume of granules  $V_{gr} = f(z)$  (dashed lines) along the length of the annular channel at different rotation frequencies  $\omega_0$ :  
 1 – 180 rpm; 2 – 150 rpm; 3 – 120 rpm

As shown in Figure 3, the shear rate of the circular flow  $\dot{\gamma}_{r\theta}$  increases proportionally to  $\omega_0$ , and the values  $\dot{\gamma}_{r\theta}$  do not depend on temperature and practically does not change along the width of the gap. As can be seen from Figure 3, the effective viscosity of the melt  $\mu_{ef}(T)$  decreases sharply along the length of the gap, which is associated with an increase in the melt temperature  $T_l = f(z)$ . In accordance with equation (21), the value  $\mu_{ef}(T)$  increases with an increase of rotation frequency  $\omega_0$  due to increasing the shear rate  $\dot{\gamma}_{r\theta}$ .



**Figure 3.** Distribution of the effective melt viscosity  $\mu_{ef}(T)$  (solid lines) and the shear speed of the tangential flow  $\dot{\gamma}_{r\theta}$  (dotted line) along the length of the annular channel at different rotation frequencies  $\omega_0$ :  
1 – 180 rpm; 2 – 150 rpm; 3 – 120 rpm

During the passage of the mixture through the channel, the granules are heated and their volume-averaged temperature  $\bar{T}_{gr}$  increases, what can be observed from Figure 4. At the rotation frequency  $\omega_0=150$  rpm the melt temperature increases by  $30^\circ\text{C}$  (Figure 2), whereas the volume-averaged temperature of the granules increases only by  $6^\circ\text{C}$ .

Figure 4 also shows the change in axial pressure along the length of the channel. At the channel length  $L_1 = 10$  mm the melt pressure decreases by 0.12 MPa. It can be observed from Figure 4 that as the melt passes through the channel, the pressure gradient  $dp/dz$  gradually decreases. According to equation (19), this is explained by the decreasing the consistency coefficient  $K_T$  with temperature.

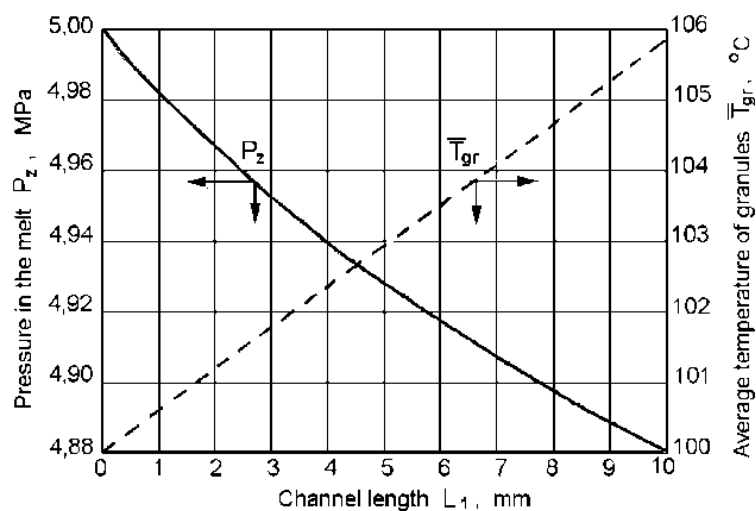


**Figure 4.** Distribution of the axial pressure  $p_z$  (solid line) and the volume-average temperature of the granules  $\bar{T}_{gr}$  (dotted line) along the length of the annular channel at the rotation frequency  $\omega_0=150$  rpm

**Conclusions.** A computational experiment has been carried out that takes into account the design characteristics of a pilot-scale disk extruder and uses a polymer composition based on high-pressure polyethylene (PE 15803-020) as a model object.

The calculation procedure is described in an analytical form and graphical dependences of the melt temperature distribution, specific volume of granules, distribution of the average temperature of the granule, and change in the effective viscosity of the melt along the channel at disk speeds of 120, 150, and 180 rpm are presented. At the disk speed from the minimum value of 120 rpm to the nominal value of 150 rpm, the temperature increases gradually, and at the disk speed of the nominal value to the maximum value of 180 rpm, the temperature increases faster.

The previously started procedure for calculating the channels of the homogenization zone has been extended.

## References

1. Kuziaiev V. M., Sviderskiy V. A., Pietukhov A.D. Modelirovaniie ekstruzii i ekstrudеров pri pererabotkie polimerov, Chast' 2. Kiev: NTUU KPI, Politehnika, 2016. 276 p.
2. Kim V. S. Teoriia i praktika ekstruzii polimerov. Moskva: Khimiia, 2005. 568 p.
3. Mikulionok I. OJ., Radchenko L. D. Modeliuvannia diskovykh ekstruderiv dlia pereroblennia polimernykh materialiv. Kyiv: NTUU, 2015. 103 p.
4. Novodvorskyi V. V., Ivanitsky G. K., Modelyuvannia techiyi rozplavu polimeru v kil'tsevomu kanali diskovoho ekstrudera. Nauka ta progres transportu. 2023. No. 1 (101). URL: <https://doi.org/10.15802/stp2023/282982>.
5. Shved M. P., Shved D. M., Novodvorskyi V. V., Kovba A. M., Protses kaskadnoyi diskovo-shesterennoyi ekstruzii ta yoho analiz. Ekolohichni nauky. 2019. No. 4 (27). P. 28–32. <https://doi.org/10.32846/2306-9716-2019-4-27-5>
6. Abeykoon C., Martin P. J., Kelley A. L., Li K., Brown E. C., Coates P. D., Investigation of the temperature homogeneity of die melt flows in polymer extrusion. Polymer Engineering and Science. 2014. No. 54 (10). P. 2430–2440. <https://doi.org/10.1002/pen.23784>
7. Wood A. K., Cleveleys T., Determination of melt temperature and velocity profiles in flowing polymer melts, 2005, Proc. 8th Brazilian Congr. Polym, 1378–1381.
8. Rauwendaal C., Estimating fully developed melt temperature in extrusion. In Conference Proceedings, 2000, 58 th SPE ANTEC. P. 307–311.
9. Rauwendaal Ch., Ponzielli G. Temperature development in screw extruders. REF, Inc. and RCT s.r.l. April 8, 2003, 16 p. URL: <http://www.rauwendaal.com>.
10. Fenot V., Bertin Y., Dorignac E., Lalizel G. A review of heat transfer between concentric rotating cylinders with or without axial flow. Int. Journ. Thermal Sciences. 2011. Vol. 50. P. 1138–1155. <https://doi.org/10.1016/j.ijthermalsci.2011.02.013>
11. Ierschov S. V., Trufanova N. M., Lukin M. D. Chislennie issliedovaniie protsessov tiecheniia rasplava polimera v kanalie zony dozirovaniia i formuiuschem instrumentie. Viestnil Piermskogo natsional'nogo issliedovatel'skogo politehnicheskogo universiteta. Maschinostroieniie. 2017. Vol. 19. No. 3. P. 163–178. <https://doi.org/10.15593/2224-9877/2017.3.10>
12. Bird R. B., Stewart W. E. Lightfoot E. N. Transport Phenomena. N.-Y., Wiley, 1960, 642 p.

## Список використаних джерел

1. Кузяев И. М., Свидерский В. А., Петухов А. Д., Моделирование экструзии и экструдеров при переработке полимеров. Часть 2. Киев: НТУУ КПИ, Политехника, 2016. 276 с.
2. Ким В. С. Теория и практика экструзии полимеров. Москва: Химия, 2005. 568 с.
3. Мікульюнок І. О., Радченко Л. Б. Моделювання дискових екструдерів для перероблення полімерних матеріалів. Київ: НТУУ «КПІ», 2015, 103 с.:
4. Новодворський В. В., Іваницький Г. К., Моделювання течії розплаву полімеру в кільцевому каналі дискового екструдера. Наука та прогрес транспорту. 2023. № 1 (101). URL: <https://doi.org/10.15802/stp2023/282982>.
5. Швед М. П., Швед Д. М., Новодворський В. В., Ковба А. М. Процес каскадної дисково-шестеренної екструзії та його аналіз. Екологічні науки. 2019. № 4 (27). С. 28–38. <https://doi.org/10.32846/2306-9716-2019-4-27-5>
6. Abeykoon C., Martin P. J., Kelley A. L., Li K., Brown E. C., Coates P. D., Investigation of the Temperature Homogeneity of Die Melt Flows in Polymer Extrusion. Polymer Engineering and Science. 2014. No. 54 (10). P. 2430–2440. <https://doi.org/10.1002/pen.23784>

7. Wood A. K., Cleveleys T., Determination of melt temperature and velocity profiles in flowing polymer melts, 2005, Proc. 8th Brazilian Congr. Polym. P. 1378–1381.
8. Rauwendaal C., Estimating fully developed melt temperature in extrusion. In Conference Proceedings, 2000, 58 th SPE ANTEC. P. 307–311.
9. Rauwendaal Ch., Ponzielli G. Temperature development in screw extruders. REF, Inc. and RCT s.r.l. April 8, 2003, 16 p. URL: <http://www.rauwendaal.com>
10. Fenot V., Bertin Y., Dorignac E., Lalizel G. A review of heat transfer between concentric rotating cylinders with or without axial flow. Int. Journ. Thermal Sciences. 2011. Vol. 50. P. 1138–1155. <https://doi.org/10.1016/j.ijthermalsci.2011.02.013>
11. Ершов С. В., Труфанова Н. М., Лукин М. Д. Численное исследование процессов течения расплава полимера в канале зоны дозирования и формирующем инструменте. Вестник ПНИПУ. Машиностроение. 2017. Т. 19. № 3. С. 163–178. <https://doi.org/10.15593/2224-9877/2017.3.10>
12. Bird R. B., Stewart W. E. Lightfoot E. N. Transport Phenomena. N.-Y.: Wiley, 1960. 642 p.

## УДК 678.023

# ЧИСЕЛЬНЕ ДОСЛІДЖЕННЯ НЕІЗОТЕРМІЧНОЇ ТЕЧІЇ РОЗПЛАВУ ПОЛІМЕРУ З НЕДОПЛАВЛЕНИМИ ГРАНУЛАМИ У ПРЯМОМУ КІЛЬЦЕВОМУ КАНАЛІ ДИСКОВОГО ЕКСТРУДЕРА

Володимир Новодворський; Георгій Іваницький; Микола Швед

Національний технічний університет України «Київський політехнічний інститут імені Ігоря Сікорського», Київ, Тернопіль

**Резюме.** Добру якість розплаву можна отримати, коли досягається механічна і температурна однорідності. Ефективним обладнанням, яке забезпечує високий рівень перемішування при невеликому перепаді тиску і відповідно незначних витратах енергії, є дисковий екструдер. Розглянуто процеси, які відбуваються в циліндричному кільцевому каналі, який починається після гвинтової нарізки. Оскільки процес проходить за дисперсійною моделлю плавлення, то в першому й другому каналах зони гомогенізації відбуваються одночасно процеси гомогенізації і доплавлення гранул, що експериментально чи теоретично ще не досліджувалося раніше в літературних джерелах. Проведено обчислювальний експеримент на основі створеної моделі течії розплаву з недоплавленими гранулами в прямому кільцевому каналі, в якому враховуються конструктивні характеристики дослідно-промислового дискового екструдера і де в якості модельного об'єкта вибрано полімерну композицію на основі поліетилену високого тиску (марки ПЕВТ 15803-020). Наведено процедуру розрахунку в аналітичній формі. Отримано графічні залежності розподілу температур розплаву, питомий об'єм гранул, розподіл середньої температури гранули та зміну ефективної в'язкості розплаву вздовж каналу при значеннях обертів диска 120, 150 та 180 об/хв. Температура розплаву збільшується поступово при частоті обертів диска від мінімального значення 120 об/хв до номінального значення 150 об/хв, а при частоті обертів диска від номінального значення до максимального – 180 об/хв. Збільшення температура відбувається швидше. Робота спрямована на дослідження дискового екструдера, який дозволяє розробити гнучкий і керований процес гомогенізації з можливістю визначати й регулювати високий рівень перемішування розплаву під час процесу екструзії за сталої продуктивності. Результати цієї роботи будуть застосовані при подальшому дослідженні неізотермічних процесів течії розплаву та плавлення гранул у конусній кільцевій та в дисковій зонах.

**Ключові слова:** дисковий екструдер, полімери, кільцеві канали, моделювання, неізотермічні процеси, плавлення.

[https://doi.org/10.33108/visnyk\\_tntu2023.04.115](https://doi.org/10.33108/visnyk_tntu2023.04.115)

Отримано 13.10.2023